01 Apr 2006

Structural and Magnetic Properties of La Mn$_{1-x}$Fe$_x$O$_3$ (0 < x < 1.0)

X.-D. Zhou
Missouri University of Science and Technology

L. R. Pederson

Qingsheng Cai

Jinbo Yang

et. al. For a complete list of authors, see https://scholarsmine.mst.edu/matsci_eng_facwork/5

Recommended Citation

Structural and magnetic properties of LaMn$_{1-x}$Fe$_x$O$_3$ (0 < x < 1.0)

X.-D. Zhou[a)] and L. R. Pederson
Pacific Northwest National Laboratory, Richland, Washington 99352

Q. Cai
Department of Physics, University of Missouri-Columbia, Columbia Missouri 65211

J. Yang, B. J. Scarfino, M. Kim, W. B. Yelon, W. J. James, and H. U. Anderson
Graduate Center for Materials Research, University of Missouri-Rolla, Rolla, Missouri 65401

C. Wang
School of Physics, Peking University, Beijing 100871, P. R. China

Electronic, structural, and magnetic properties of Mn-doped lanthanum ferrites were studied by neutron diffraction, superconducting quantum interference device, and impedance spectroscopy. Neutron diffraction refinements were performed with the constraint of full La occupancy, which showed the presence of excess oxygen when $x < 0.4$. Mixed valent Mn cations and cation vacancies, therefore, exist in all the samples. The samples with $x > 0.7$ are magnetically ordered at room temperature with orthorhombic symmetry (*Pbnm*). When $x < 0.3$ the structure is rhombohedral and magnetically disordered above 16 K. The majority carriers, electron holes, correspond to high oxidation states of Mn. The carrier concentration is determined from the Seebeck coefficients, and is a function of temperature and Fe concentration. The measurements of conductivity and Seebeck coefficients show polaron hopping at elevated temperatures. © *2006 American Institute of Physics.* [DOI: 10.1063/1.2176389]

INTRODUCTION

Extensive studies have been made on perovskite oxides (ABO$_3$) containing Mn ions since the discovery of "colossal" magnetoresistance (CMR) effects.[1,2] Much attention has been paid to the generic composition as; $R_{1-x}A'_x$MnO$_3$, where R is a rare earth cation and A' represents alkaline earth cations. Both a polaron effect arising from the Jahn-Teller distortion and double exchange were assumed to contribute to large magnetoresistance exhibited for $0.2 \leq x \leq 0.4$.[3,4] In addition to the CMR effect, substitution of B site cations is of interest, with other transition metal ions replacing Mn.

Raffaelle *et al.* observed a deep conductivity minimum near $x=0.05$ in La(Cr$_{1-x}$Mn$_x$)O$_3$ and a nearly constant carrier concentration at $x > 0.6$ at 1300 K.[5,6] Multiple trapping was used to explain the phenomena for the small x and charge disproportionation was assumed to be responsible for the behavior for $x > 0.6$. The magnetic interaction is of particular interest in the B site doped LaMnO$_{3+\delta}$ because of many possible exchange interactions. Since the La–O sublattice is homogenous, it does not create a random Coulomb potential.[7] Of the many possible B site dopants including Cr,[5] Co,[8] and Ni,[9] doping with Fe into LaMnO$_3$ results in unique properties, particularly the suppression of ferromagnetism and conductivity with increasing concentration of Fe^{3+} ions.

Tong *et al.* reported the presence of a paramagnetic-ferromagnetic transition in LaMn$_{1-x}$Fe$_x$O$_3$ ($x \leq 0.4$) without an insulator-metal transition.[7] A ferromagnetic coupling between Fe and Mn ions was observed from ESR spectra, from which they assumed the existence of the double exchange interaction between the Fe ions and Mn ions and an intermediate spin state of Fe^{3+} ($t_{2g}^4 e_g^1$). Very recently, Shekhar *et al.*[10] reported that the appearance of ferromagnetism in LaMn$_{0.5}$Fe$_{0.5}$O$_3$ was a result of processing techniques. Ferromagnetic or antiferromagnetic (AFM) characteristics exist with the presence of Mn-rich and/or Fe-rich clusters in LaMn$_{0.5}$Fe$_{0.5}$O$_3$, whereas uniform distribution of Fe and Mn ions results in nonmagnetic behavior.

In this paper, neutron diffraction is used to study the structure and AFM properties of La(Mn$_{1-x}$Fe$_x$)O$_3$ over a wide range of compositions $(0 < x < 1)$. Additionally, low temperature magnetic and high temperature electrical properties are reported.

EXPERIMENT

The raw powders were synthesized using the glycine nitrate method,[11] followed by calcining, uniaxial pressing, and sintering. The powder neutron diffraction was performed at the University of Missouri Research Reactor on the specimens calcined at 1000 °C in air, using the position sensitive detector diffractometer. The Rietveld refinement was carried out using the FULLPROF code,[12] which permits both multiphase and magnetic structure refinements. The temperature dependence of magnetization under both zero field cooling (ZFC) and 0.01 T field cooling (FC) conditions was measured by a superconducting quantum interference device (SQUID) magnetometry. For the electrical measurements, the rectangular samples $(2.00 \times 0.20 \times 0.20$ cm^3) were sintered at 1250 °C for 2 h with a ramping rate of 3 °C/min. The final density of these specimens was more than 90% of the theoretical values. A four-point-probe technique was used
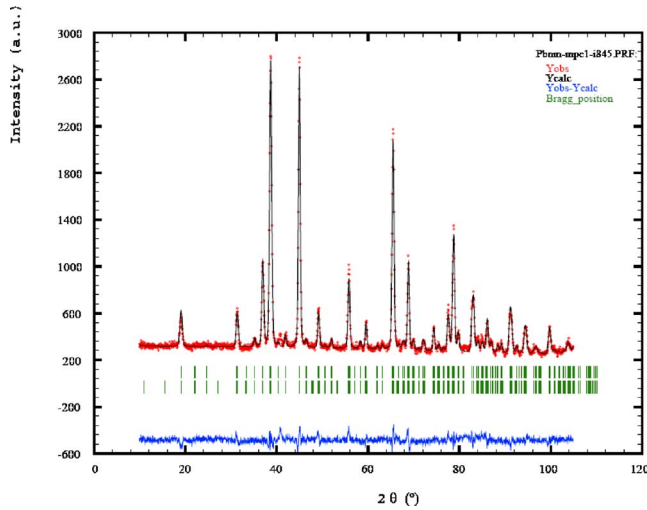
———————
[a)]Electronic mail: zhou@umr.edu

FIG. 1. (Color online) Neutron diffraction pattern for $LaMn_{0.50}Fe_{0.50}O_3$ at 16 K.

to measure electrical resistance in the temperature range 150–1000 °C. Thermoelectric power was measured on a similar rectangular sample, which was corrected by considering absolute thermopower for platinum to yield the Seebeck coefficient of the sample.

RESULTS AND DISCUSSION

Initial experiments were focused on both x-ray diffraction (XRD) and neutron diffraction (ND) measurements on samples of $LaFe_{1-x}Mn_xO_{3+\delta}$, for $0.05 \leq x \leq 0.95$. Low temperature neutron diffraction measurements were carried out at 16 K. Both XRD and neutron diffraction indicated that all samples were single phase. Shown Fig. 1 is the ND to support this conclusion. The Rietveld refinements were performed on neutron diffraction data with the constraint of full La occupancy and La/(Mn+Fe) equal to one.[13–15] The Oxygen site occupancy, therefore, was allowed to vary. Lattice parameters and oxygen occupancy are listed in Table I. The crystal structure of the end composition, $LaMnO_{3+\delta}$, is rhombohedral when $\delta > 0.1$, typically calcined at low temperature and/or in O_2; whereas it is orthorhombic for $LaFeO_3$. As expected, the Fe-rich samples ($x \geq 0.5$) have orthorhombic

symmetry and the data were refined in space group *Pbnm*. Likewise, the Mn-rich samples have rhombohedral symmetry (space group $R3/c$).

During the processing of Mn-doped lanthanum ferrites (LMFO) powders, the ratio of La/(Fe+Mn) was set at 1 in the precursor solution. The chelation and combustion in glycine nitrate process creates local homogeneity of cation distribution. It is, therefore, reasonable to put the constraint of La/(Mn+Fe) equal to one and allow the oxygen occupancy to vary. The refinement of the oxygen content shows the presence of oxygen excess, particularly when $x < 0.5$ (i.e., Mn-rich samples). For $x = 0.95$, the oxygen excess is negligible, while for $x = 0.05$ the excess reaches 7.5%. Perovskite is a close packed structure, thus interstitial oxygen is not allowed. In addition, the oxygen content is refined for the nominal site, which indicates the existence of cation vacancies on both the A and B sublattices. The amount of oxygen excess (or cation vacancies) is of substantial importance in manganites, not only on the structural properties, but also on the electrical and magnetic properties. When the cation vacancies are present, the charge neutrality condition necessitates an increasing oxidation state of some Mn ions from Mn^{3+} to Mn^{4+} which governs the magnetic and electronic behavior in manganites.

The four samples with $x \geq 0.6$ (Fe rich) are found to be magnetically ordered at room temperature. Magnetic moments increase with increasing x. It is of interest to compare LMFO with $La_{1-x}Sr_xFeO_3$, whose Néel temperature decreases with increasing Sr concentration and decreasing oxygen occupancy with a linear relation between magnetic moment (16 K) and Fe^{3+} concentration being observed in $La_{0.60}Sr_{0.40}FeO_{3-\delta}$.[16] Shown in Fig. 2 is a plot of magnetic moment at 16 K as a function of Fe concentration. A linear relation (dot line) is included as a comparison. When $x > 0.6$, the refined magnetic moment is greater than from the linear approximation, whereas when $x < 0.6$ the refined magnetic moment is much smaller. The superexchange interaction of Fe–O–Mn was assumed to be the one of the strongest in perovskites containing $3d$ transition metal ions. Since cation vacancies are negligible when $x > 0.6$, the majority B site cations are Fe^{3+} and Mn^{3+}. Results from Fig. 2 indicate Fe–O–Mn superexchange may exist and contribute to the overall

TABLE I. Room temperature structural parameters, antiferromagnetic moment per Fe, unit cell volume, and the goodness of Fit of $La(Mn_{1-x}Fe_x)O_{3+\delta}$. Rietveld refinements were carried out using the constraints of A/B ratio being 1 (Ref. 18).

| x	Space group	a (Å)	b (Å)	c (Å)	Volume (Å³)	AFM (μ_B) RT
0.05	$R\bar{3}c$	5.518 74	5.518 74	13.3256	351.476	$\cdots$
0.1	$R\bar{3}c$	5.519 21	5.519 21	13.3305	351.665	$\cdots$
0.2	$R\bar{3}c$	5.521 38	5.521 38	13.337 13	352.118	$\cdots$
0.4	$R\bar{3}c$	5.522 82	5.522 82	13.3709	353.193	$\cdots$
0.5	*Pbnm*	5.538 34	5.501 02	7.797 42	237.56	$\cdots$
0.6	*Pbnm*	5.537 18	5.5073	7.820 86	238.496	1.67
0.8	*Pbnm*	5.556 46	5.5384	7.832 53	241.038	2.82
0.9	*Pbnm*	5.553 07	5.553 67	7.843 86	241.904	3.33
0.95	*Pbnm*	5.545 28	5.557 85	7.860 89	242.271	3.49
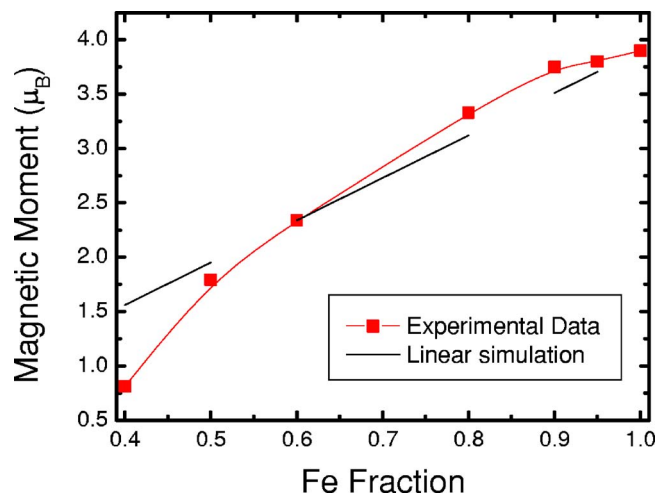
FIG. 2. (Color online) Magnetic moment (16 K) as a function of Fe fraction for $LaMn_{1-x}Fe_xO_3$.

AFM moment; but the Fe–O–Fe superexchange interaction dominates the magnetic properties when $x > 0.6$.

The antiferromagnetism was significantly weakened with increasing Mn content. When $x = 0.4$, the expected AFM moment is around $1.5\mu_B$ assuming superexchange interaction between Fe^{3+} ions and O^{2-} ions. A much lower AFM moment of $0.81\mu_B$ was observed. At first, one may conclude that this behavior is due to a segregation of Fe^{3+} ions from Mn ions. Cation vacancies due to excess of oxygen, however, must be taken into consideration. The M-T curves were measured under both ZFC and 0.01 T FC. The T_{onset} is defined as the temperature corresponding to the crossing point of the PM line and tangent line on the PM-FM transition region. There exists a PM-FM (or AFM) transition at low temperature for all samples. In the samples with $x \le 0.6$, the trend of ZFC is very different from that of FC, which indicates the formation of spin-glass clusters. The T_C decreases as the doping level increases. Shekhar *et al.*[10] observed that the magnetization and T_{onset} decreased with reduced annealing temperature, which indicates the presence of spin-glass clusters in the samples annealed at relatively low temperatures. The magnetization curves in this study are similar to those reported in the literature.

In terms of magnetic exchange mechanism, De *et al.*[17] proposed both a predominant ferromagnetic interaction for $x < 0.15$ and a competition between ferromagnetism and AFM when $x \sim 0.3$. Furthermore, they assumed that the mechanism varied discontinuously for $x > 0.5$. From the present study, we find that an AFM superexchange interaction dominates when $x \ge 0.5$; whereas for $x \le 0.5$, the magnetic interaction is highly correlated with the cation vacancy concentration (oxygen excess). Furthermore, we conducted measurements of both high temperature electrical conductivity and the Seebeck coefficient, which can provide information about carrier formation, concentration and transport in this series of samples. It is found that the carrier concentra-

tion increases with increasing temperature, indicating that carrier formation is a thermally activated process. The carrier concentration becomes stable at ~ 0.4 when $T > 800°$, which indicates that Fe ions are at 2+ and act as the dopants at the elevated temperatures. Detailed results will be published elsewhere.

CONCLUSION

Measurements of neutron diffraction, SQUID, and impedance spectroscopy were conducted on $LaMn_{1-x}Fe_xO_{3+\delta}$ ($0.05 \le x \le 0.95$). An orthorhombic phase was observed for $x \ge 0.50$, whereas the rhombohedral symmetry was observed for $x \le 0.40$ with the existence of oxygen excess (or cation vacancies). Refinement of neutron diffraction results showed a decreasing saturation magnetic moment with reduced Fe concentration. An AFM superexchange interaction dominates when $x \ge 0.5$; whereas for $x \le 0.5$, the magnetic interaction is highly correlated with the cation vacancy concentration. Results in this study show that Mn-rich samples favor double exchange, whereas Fe-rich samples favor superexchange.

[1]R. von Helmolt, J. Wecker, B. Holzapfel, L. Schultz, and K. Samwer, Phys. Rev. Lett. **71**, 2331 (1993).
[2]S. Jin, T. H. Tiefel, M. McCormack, R. A. Fastnacht, R. Ramesh, and L. H. Chen, Science **264**, 413 (1994).
[3]a. J. Millis, P. B. Littlewood, and B. I. Shraiman, Phys. Rev. Lett. **74**, 5144 (1995).
[4]C. Zener, Phys. Rev. **82**, 403 (1951).
[5]R. Raffaelle, H. U. Anderson, D. M. Sparlin, and P. E. Parris, Phys. Rev. Lett. **65**, 1383 (1990).
[6]R. Raffaelle, H. U. Anderson, D. M. Sparlin, and P. E. Parris, Phys. Rev. B **43**, 7991 (1991).
[7]W. Tong, B. Zhang, S. Tan, and Y. Zhang, Phys. Rev. B **70**, 014422 (2004).
[8]J. Goodenough, A. Wold, R. J. Arnott, and N. Menyuk, Phys. Rev. **124**, 373 (1961).
[9]A. Wold, R. J. Arnott, and J. B. Goodenough, J. Appl. Phys. **29**, 387 (1958).
[10]S. D. Bhame, V. L. J. Joly, and P. A. Joy, Phys. Rev. B **72**, 054426 (2005).
[11]L. A. Chick, L. R. Pederson, G. D. Maupin, J. L. Bates, L. E. Thomas, and G. J. Exarhos, Mater. Lett. **10**, 6 (1990).
[12]J. Rodriguez-Carvajal, FULLPROF program, Version 3.d (1998).
[13]K. Hirota, S. Ishihara, H. Fujioka, M. Kubota, H. Yoshizawa, Y. Moritomo, Y. Endoh, and S. Maekawa, Phys. Rev. B **65**, 064414 (2002).
[14]J. Topfer, and J. B. Goodenough, Chem. Mater. **9**, 1467 (1997).
[15]J. Topfer and J. B. Goodenough, J. Solid State Chem. **130**, 117 (1997).
[16]X.-D. Zhou, Q. Cai, J. Yang, M. Kim, W. B. Yelon, W. J. James, Y.-W. Shin, B. J. Scarfino, and H. U. Anderson, J. Appl. Phys. **97**, 10C314 (2005).
[17]K. De, R. Ray, R. N. Panda, S. Giri, H. Nakamura, and T. Kohara, J. Magn. Magn. Mater. **288**, 339 (2005).
[18]J. B. Yang, W. B. Yelon, W. J. James, Z. Chu, M. Kornecki, Y. X. Xie, X. D. Zhou, H. U. Anderson, A. G. Joshi, and S. K. Malik, Phys. Rev. B **66**, 184415 (2002).